

## Laser spectroscopy of gas confined in nanoporous materials

Tomas Svensson<sup>1,a)</sup> and Zhijian Shen<sup>2</sup>

<sup>1</sup>*Department of Physics, Division of Atomic Physics, Lund University, 221 00 Lund, Sweden*

<sup>2</sup>*Department of Physical, Inorganic, and Structural Chemistry, Arrhenius Laboratory, Stockholm University, 106 91 Stockholm, Sweden and Berzelii center EXSELENT on porous materials, Stockholm University, 106 91 Stockholm, Sweden*

(Received 23 September 2009; accepted 22 December 2009; published online 13 January 2010)

We show that high-resolution laser spectroscopy can probe surface interactions of gas confined in nanocavities of porous materials. We report on strong line broadening and unfamiliar line shapes due to tight confinement, as well as signal enhancement due to multiple photon scattering. This new domain of laser spectroscopy constitute a challenge for the theory of collisions and spectroscopic line shapes, and open for new ways of analyzing porous materials and processes taking place therein. © 2010 American Institute of Physics. [doi:10.1063/1.3292210]

The tight confinement and large surface-areas offered by nanoporous materials give rise to numerous interesting and useful phenomena. Important topics in this vast and rapidly advancing field include storage of carbon dioxide and hydrogen,<sup>1,2</sup> molecular sieving,<sup>3</sup> catalysis,<sup>4,5</sup> ion exchange, melting and freezing under confinement,<sup>6</sup> luminescence of porous silicon,<sup>7</sup> and chemical sensing. The interactions between gases and porous materials are often of particular interest. However, due to lack of methodologies, many processes occurring inside nanoporous structures are not fully understood.

Here, we show that the high-resolution laser absorption spectroscopy allows sensing of gases confined in nanocavities of porous materials and investigation of the gas-surface interactions. We report that the tight confinement, i.e., frequent surface interactions, results in strong (gigahertz) line broadening and unfamiliar line shapes. Severe multiple scattering, and the corresponding long photon path lengths, enhance our signals and makes it possible to study weak transitions and thin samples. The interpretation of observed high-resolution spectra constitutes a new challenge for the theory of collisions and spectroscopic line shapes. This unexplored domain of laser spectroscopy envisages new ways for studying important processes occurring in nanoporous materials, such as gas adsorption, gas transport, heterogenous catalysis, and van der Waal interactions between surfaces and molecules. In addition, nanoporous materials may be an interesting system for fundamental studies of hard collisions and corresponding effects on molecular spectra. Finally, as the line broadening is shown to depend heavily on the pore size, our work reveals a new, nondestructive technique for pore size assessment.

Laser-based sensing of gas in porous media has been pursued since 2001.<sup>8</sup> In this work, we have studied molecular oxygen (O<sub>2</sub>) located in subwavelength pores of nanoporous bulk alumina (Al<sub>2</sub>O<sub>3</sub>). Measurements have been conducted on two materials with different pore size distribution, both carefully characterized using mercury intrusion porosimetry.<sup>9</sup> The first is an  $\alpha$ -alumina ceramic manufactured by sintering a monodisperse 0.3  $\mu$ m  $\alpha$ -alumina powder at 1000 °C. The resulting cylindrical samples are 13 mm in diameter with a thickness up to 6 mm, having a narrow ( $\pm 10$  nm) pore

size distribution centered around 70 nm and a total porosity of 35%. The second material is a  $\gamma$ -alumina ceramic prepared by means of spark plasma sintering, yielding a 2.2 mm thick, 12 mm diameter sample with pore sizes of  $18 \pm 2$  nm and a total porosity of 50%.

In order to sense and probe oxygen confined in these turbid materials, we utilize the R9Q10 line (760.654 nm) of the near infrared A-band of O<sub>2</sub>. The transition is electric dipole forbidden and weak, having a line strength of about  $2.6 \times 10^{-13}$  cm<sup>2</sup> Hz at room temperature.<sup>10</sup> At atmospheric conditions (1 atm, 300 K, and 20.9% O<sub>2</sub>), this results in a peak absorption coefficient of  $2.7 \times 10^{-4}$  cm<sup>-1</sup> and a half width at half maximum (HWHM) ( $\Gamma$ ) of 1.6 GHz (a 0.4 GHz Doppler component together with a 1.5 GHz pressure broadening, yielding a Voigt profile that can be approximated by a Lorentz profile).

Our spectroscopic instrumentation is based on high-resolution tunable diode laser absorption spectroscopy, and wavelength modulation spectroscopy (WMS) is employed when higher sensitivity is needed. A detailed description of the instrumentation is available elsewhere.<sup>11</sup> Briefly, the output from a 0.3 mW tunable single-mode vertical-cavity surface-emitting diode laser is injected centrally into the porous solid, and the diffuse transmission is detected by a  $5.6 \times 5.6$  mm<sup>2</sup> large-area photodiode. All measurements are carried out under atmospheric conditions, and WMS experiments are conducted using an optical frequency modulation amplitude of  $2.2 \times 1.6$  GHz (i.e., maximizing then second harmonic WMS signal of free oxygen). Speckle noise is a severe problem, but is suppressed by employing mechanical dithering and averaging.<sup>12</sup>

Since the strength of the gas absorption imprint is proportional to the path length through pores, the scattering properties of the samples are of paramount importance. We have measured the optical properties of our samples by employing photon time-of-flight spectroscopy (PTOFS).<sup>13</sup> We inject short (picosecond) light pulses centrally into the cylindrical samples using a 600  $\mu$ m optical fiber, and collect the transmitted and broadened pulses on the other side using a second fiber. The measurement gives us direct information on the photon time-of-flight (TOF) distribution. Using a volume averaged refractive index, one can estimate the corresponding path lengths, and the theory of photon diffusion can be used to determine reduced scattering coefficients. Figure 1 shows the scattering properties of our two alumina materials.

<sup>a)</sup>Electronic mail: tomas.svensson@fysik.lth.se.

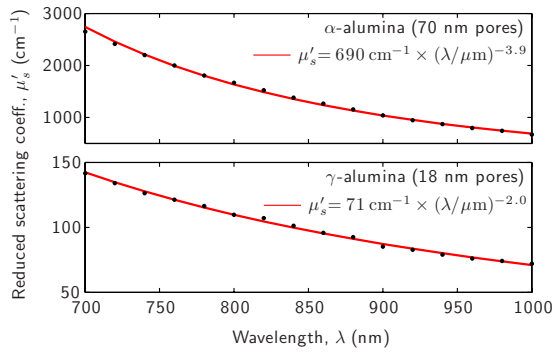


FIG. 1. (Color online) Reduced scattering coefficients of the two alumina materials (pore diameters of 70 and 18 nm, respectively). At 760 nm, the difference in scattering is a factor 16 ( $2000 \text{ cm}^{-1}$  against  $120 \text{ cm}^{-1}$ ). Interestingly, the sample with the larger pores exhibit a  $\lambda^{-4}$  Rayleigh-type scattering decay, while the sample with the smaller pores only show a  $\lambda^{-2}$  behavior. This suggests that the major scattering contribution in the latter sample originates from collective effects rather than from individual 18 nm pores.

The  $\alpha$ -alumina exhibits extremely strong scattering, having a reduced scattering coefficient at 760 nm of about  $2000 \text{ cm}^{-1}$ . This means that the light propagation can be thought of as a random walk of photons being isotropically scattered on an average of each  $5 \mu\text{m}$ . For a 2 mm  $\alpha$ -alumina sample, the average TOF was about 1.4 ns, corresponding to a total path length of 28 cm. The average path length is proportional to the square of the thickness, and should therefore be about 250 cm for a 6 mm thick sample. Such long path lengths allows us to study the direct oxygen absorption, and show that this and similar materials can be used as gas cells, for e.g., sensing applications. Figure 2 shows the experimental spectrum of  $\text{O}_2$  confined in the 70 nm diameter pores of a 6 mm thick  $\alpha$ -alumina, and compares it to a measurement on free oxygen (a 23 cm path through ambient air). Data evaluation involves simultaneous fitting of a linear baseline and a superimposed Lorentzian line shape. While experiments on free oxygen are in good agreement with expected line parameters, oxygen confined in the  $\alpha$ -alumina exhibit a significantly broader spectrum (2.3 GHz HWHM, compared to 1.6 GHz for free oxygen). Although

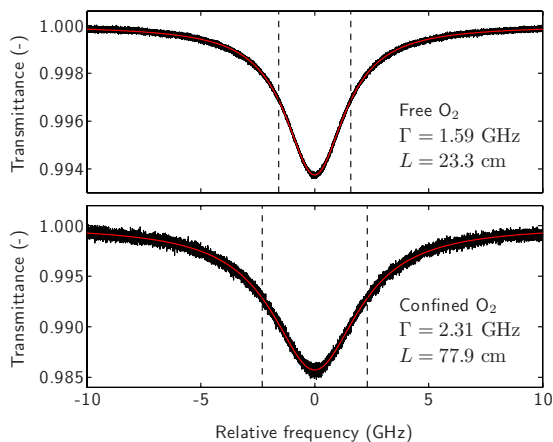


FIG. 2. (Color online) Comparison of experimental line shapes of free oxygen and oxygen confined in 70 nm pores of  $\alpha$ -alumina. Lorentzian profiles (red, smooth) are fitted to experimental data (black, noisy). Fitted line shape halfwidths,  $\Gamma$ , are stated in the graph and marked by vertical dashed lines. The fitted path length through pores,  $L$ , assumes an oxygen concentration of 20.9%. For the  $\alpha$ -alumina sample, the detected power was  $0.8 \mu\text{W}$ .

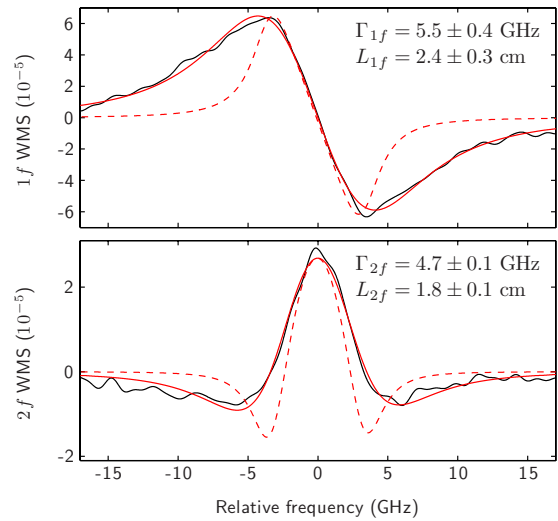


FIG. 3. (Color online) Intensity corrected WMS signals obtained from the  $\gamma$ -alumina sample with 18 nm pore diameters (noisy, black solid) together with fitted WMS simulations for Lorentzian line shapes (smooth, red solid). The detected power was  $3 \mu\text{W}$ . The tight confinement causes significant line broadening, here illustrated by a comparison to normalized WMS signals of free oxygen (dashed red,  $\Gamma = 1.6 \text{ GHz}$ ). Stated HWHM ( $\Gamma$ ) and path length through pores ( $L$ ) refer to fitted values (mean  $\pm$  standard deviation of three repetitions). Note the discrepancy in fitted values between first and second harmonic, showing that a Lorentzian is an improper line shape model.

mercury intrusion porosimetry already have shown that the material has an open porosity, we double checked this issue by flushing the sample with nitrogen. The oxygen imprint vanished completely almost instantaneously, further proving that we are not measuring oxygen in closed pores with elevated pressures. Note also that the fitted path length of 78 cm through gas is in good agreement with the PTOFS data (about  $\phi_\alpha = 35\%$  of the total 250 cm path length should be through pores).

The lower scattering of the  $\gamma$ -alumina sample makes gas sensing more challenging. The average TOF at 760 nm was 120 ps, corresponding to a total path length of about 3 cm. The corresponding peak absorption fraction due to oxygen is of the order of  $10^{-4}$  or less. To be able to study such a weak absorption, we were forced to employ WMS. While increasing sensitivity, WMS renders line shape analysis less straightforward. Furthermore, in order to eliminate non-negligible oxygen absorption originating from optical path outside the sample, WMS measurements were made in a differential manner (the offset is determined by measuring on a nonporous turbid solid of equal thickness). Figure 3 shows the resulting first ( $1f$ ) and second ( $2f$ ) WMS harmonics together with separately fitted WMS simulations. The tight confinement is now the dominating source of line broadening. The linewidth is about 5 GHz, by far exceeding the 1.6 GHz exhibited by free oxygen at atmospheric pressure. In addition, the data is persistently not well fitted by a Lorentzian model. This is most prominent in  $2f$  where, in comparison with a Lorentzian response, the observed WMS feature exhibit a sharper and higher main peak in combination with less pronounced negative side-peaks. The bad  $2f$  fit and the major discrepancy in fitted HWHM ( $\Gamma$ ) and path length ( $L$ ) shows that a Lorentzian is an improper line shape model. In contrast, similar WMS experiments on the  $\alpha$ -alumina (where the Lorentzian contribution from pressure broadening domi-

nates) results in minor differences between  $1f$  and  $2f$  (less than 2% and 7% difference in  $\Gamma$  and  $L$ , respectively), and a HWHM in good agreement with the direct transmittance shown in Fig. 2.

As intermolecular collisions is known to be a strong source of line broadening, it is natural to investigate whether wall collisions may explain the broadening exhibited by these tightly confined oxygen molecules. In fact, the mean free path of  $O_2$  in air at atmospheric pressure is about 60 nm. Nanoconfinement may thus render wall collisions and intermolecular collisions comparable sources of broadening. Broadening of spectral lines due to wall collisions have previously been discussed for the case of low pressure microwave spectroscopy. There, investigations in the milli-Torr regime ( $10^{-6}$  atmospheres) renders the mean free path comparable to the size of the utilized gas cells (i.e., centimeter scale). The exact nature of the broadening mechanism was the subject of a lively discussion.<sup>14–16</sup> According to classical gas kinetics, the rate  $f_{\text{wall}}$  at which molecules in an ideal gas collides with the walls of its container as follows:

$$f_{\text{wall}} = \frac{1}{\tau_{\text{wall}}} = \frac{A}{V} \sqrt{\frac{kT}{2\pi m}} = \frac{A}{4V} \times v_{\text{avg}}, \quad (1)$$

where  $\tau_{\text{wall}}$  is the average time between wall collisions,  $A$  the container area,  $V$  the volume,  $k$  the Boltzmann constant,  $T$  the temperature,  $m$  the molecular mass, and  $v_{\text{avg}}$  the average speed of the molecules (450 nm/ns at 300 K for  $O_2$ ). It was first “tacitly” assumed that wall collision gave rise to a Lorentzian component with a HWHM  $\Delta\nu$  given by  $1/2\pi\tau_{\text{wall}}$ , but it was later shown that the line shape is not Lorentzian and that it depends on the container shape.<sup>16,17</sup> It is thus not surprising that Lorentzian simulations failed to explain the line shapes exhibited by oxygen confined in the  $\gamma$ -alumina.

In contrast to microwave spectroscopy, where reported levels of wall broadening were in the kilohertz range, our experiments show that molecules confined in nanopores exhibit broadening in the gigahertz range, i.e., a factor  $10^6$  stronger. A theoretical estimation is given by employing  $\Delta\nu = 1/2\pi\tau$  in combination with the outcome of Eq. (1), for e.g., spherical cavities. For 70 and 18 nm sphere diameters, the procedure yields  $\Delta\nu$ 's of 1.5 and 6 GHz, respectively. However, since the pore size given by mercury intrusion porosimetry reflects the most narrow passages in the pore structure,<sup>9</sup> we expect a less pronounced wall collision broadening. Given the uncertainty in effective pore size, and that the wall collision line shape is unknown, it is difficult to analyze the observed linewidths in more detail. Nonetheless, these basic calculations show that the observed broadening is in reasonable agreement with theory of wall collisions. On the other hand, we have not yet been able to explain the discrepancy between WMS harmonics. Further works on line shape theory for confined molecules are thus needed.

It should be noted that all measurements described above was conducted at atmospheric pressure. In contrast to intermolecular broadening, broadening due to wall interactions is pressure independent. It is thus possible to further isolate the phenomenon by performing experiments under reduced pressures. This will allow more careful analysis of line shapes, as well as investigations of surface interactions in larger pores of macroporous materials. In fact, broadening due to wall collisions in micrometer-sized cavities was recently encoun-

tered in connection to low pressure spectroscopy of gas confined in the 10  $\mu\text{m}$  core of photonic crystal fibers.<sup>18,19</sup> Besides being of fundamental physical interest, broadening due to wall collisions can also be used for nondestructive assessment of effective pore size. Furthermore, although no line shift was observed in our experiments, van der Waals interactions between surfaces and atoms or molecules may be an important effect if our experiments are extended to the study of other gases or vapors. Line shifts due to coupling between atomic vapors and solid surfaces has been demonstrated for atomic beams passing close to surfaces,<sup>20</sup> as well as for vapors confined in so called “extremely thin cells.”<sup>21,22</sup> Similar experiments made on gases confined in porous materials may be of great value for the understanding of the interaction between gases and surfaces of porous materials. Another aspect not yet mentioned is Dicke narrowing,<sup>23</sup> which has been shown to be influenced by the interaction with surfaces and atoms.<sup>24</sup> Its relation to our experiments on gases in porous materials remains an open question.

This work was funded by the Swedish Research Council via Professor Stefan Andersson-Engels (Grant No. VR 2007-4214). Dr. Mats Andersson, Dr. Lars Rippe, M.Sc. Erik Alerstam, Dr. Dmitry Khoptyar, Professor Stefan Kröll, Professor Sune Svanberg, and Professor Stefan Andersson-Engels are acknowledged for fruitful discussions and/or collaboration on spectroscopic instrumentation. Karin Lindqvist at Swerea IVF is acknowledged for preparing the  $\alpha$ -alumina.

<sup>1</sup>N. L. Rosi, J. Eckert, M. Eddaoudi, D. T. Vodak, J. Kim, M. O’Keeffe, and O. M. Yaghi, *Science* **300**, 1127 (2003).

<sup>2</sup>B. Wang, A. P. Cote, H. Furukawa, M. O’Keeffe, and O. M. Yaghi, *Nature (London)* **453**, 207 (2008).

<sup>3</sup>M. Davis, *Nature (London)* **417**, 813 (2002).

<sup>4</sup>A. Corma, *Chem. Rev. (Washington, D.C.)* **97**, 2373 (1997).

<sup>5</sup>J. M. Thomas, R. Raja, G. Sankar, and R. G. Bell, *Nature (London)* **398**, 227 (1999).

<sup>6</sup>H. K. Christenson, *J. Phys.: Condens. Matter* **13**, R95 (2001).

<sup>7</sup>L. T. Canham, *Appl. Phys. Lett.* **57**, 1046 (1990).

<sup>8</sup>M. Sjöholm, G. Somesfalean, J. Alnis, S. Andersson-Engels, and S. Svanberg, *Opt. Lett.* **26**, 16 (2001).

<sup>9</sup>J. Rouquerol, D. Avnir, C. W. Fairbridge, D. H. Everett, J. H. Haynes, N. Pernicone, J. D. F. Ramsay, K. S. W. Sing, and K. K. Unger, *Pure Appl. Chem.* **66**, 1739 (1994).

<sup>10</sup>A. Predoi-Cross, K. Harnbrook, R. Keller, C. Povey, I. Schofield, D. Hurtmans, H. Over, and G. C. Mellau, *J. Mol. Spectrosc.* **248**, 85 (2008).

<sup>11</sup>T. Svensson, M. Andersson, L. Rippe, S. Svanberg, S. Andersson-Engels, J. Johansson, and S. Folestad, *Appl. Phys. B: Lasers Opt.* **90**, 345 (2008).

<sup>12</sup>T. Svensson, M. Andersson, L. Rippe, J. Johansson, S. Folestad, and S. Andersson-Engels, *Opt. Lett.* **33**, 80 (2008).

<sup>13</sup>T. Svensson, E. Alerstam, D. Khoptyar, J. Johansson, S. Folestad, and S. Andersson-Engels, *Rev. Sci. Instrum.* **80**, 063105 (2009).

<sup>14</sup>W. Gordy, *Rev. Mod. Phys.* **20**, 668 (1948).

<sup>15</sup>R. H. Johnson and M. W. P. Strandberg, *Phys. Rev.* **86**, 811 (1952).

<sup>16</sup>M. Danos and S. Geschwind, *Phys. Rev.* **91**, 1159 (1953).

<sup>17</sup>S. C. M. Luijendijk *J. Phys. B* **8**, 2995 (1975).

<sup>18</sup>S. Ghosh, J. E. Sharping, D. G. Ouzounov, and A. L. Gaeta, *Phys. Rev. Lett.* **94**, 093902 (2005).

<sup>19</sup>J. Hald, J. C. Petersen, and J. Henningsen, *Phys. Rev. Lett.* **98**, 213902 (2007).

<sup>20</sup>V. Sandoghdar, C. I. Sukenik, E. A. Hinds, and S. Haroche, *Phys. Rev. Lett.* **68**, 3432 (1992).

<sup>21</sup>I. Maurin, P. Todorov, I. Hamdi, A. Yarovitskiy, G. Dutier, D. Sarkisyan, S. Saliel, M.-P. Gorza, M. Fichet, D. Bloch, and M. Ducloy, *J. Phys.: Conf. Ser.* **19**, 20 (2005).

<sup>22</sup>M. Fichet, G. Dutier, A. Yarovitskiy, P. Todorov, I. Hamdi, I. Maurin, S. Saliel, D. Sarkisyan, M.-P. Gorza, D. Bloch, and M. Ducloy, *Europhys. Lett.* **77**, 54001 (2007).

<sup>23</sup>R. Dicke, *Phys. Rev.* **89**, 472 (1953).

<sup>24</sup>R. P. Frueholz and J. C. Camparo, *Phys. Rev. A* **35**, 3768 (1987).